Critical evaluation of the computational methods used in the forced polymer translocation

V. V. Lehtola, R. P. Linna, and K. Kaski
Department of Biomedical Engineering and Computational Science, Helsinki University of Technology, P. O. Box 9203, FIN-02150 TKK, Finland

(Received 19 June 2008; revised manuscript received 24 October 2008; published 29 December 2008)

In forced polymer translocation, the average translocation time τ scales with respect to pore force f and polymer length N as $\tau \sim f^{-1}N^{\beta}$. We demonstrate that an artifact in the Metropolis Monte Carlo method resulting in breakage of the force scaling with large f may be responsible for some of the controversies between different computationally obtained results and also between computational and experimental results. Using Langevin dynamics simulations we show that the scaling exponent $\beta \leqslant 1+\nu$ is not universal, but depends on f. Moreover, we show that forced translocation can be described by a relatively simple force balance argument and β to arise solely from the initial polymer configuration.

DOI: 10.1103/PhysRevE.78.061803 PACS number(s): 36.20.Ey, 87.15.La

I. INTRODUCTION

The force-driven transport of biopolymers through a nanoscale pore in a membrane is a ubiquitous process in biology. Despite the complex dynamics involved in the process, the Monte Carlo (MC) method has been almost the only computational method used for modeling it; see the schematic Fig. 1. Only fairly recently more realistic dynamics have been applied [1–5]. The classic theoretical treatment based on writing down the free energy for a system of two equilibrium ensembles separated by a wall [6,7], henceforth called Brownian translocation, has not found support from MC simulations. The close-to-equilibrium dynamics would validate the derivation of the translocation dynamics using the Rouse relaxation time or diffusion based arguments. The validity of assumptions about the diffusion constant along the polymer chain was questioned already by the authors of [8,9], who also noted that the characteristic translocation time both for phantom and self-avoiding polymer chains was bound to be greater than their characteristic time for relaxation to thermal equilibrium. The theoretical treatment of forced translocation can be said to have so far been almost solely guided by MC simulations [10,11], despite the MC results contradicting the available experimental results. Hence the theory has evolved independently of the experimental findings.

In the attempt to determine the dynamical universality of translocation processes the scaling of the average translocation time τ with respect to the polymer chain length N as $\tau \sim N^{\beta}$ has been under intensive study. There is an abundance of research reporting different scaling exponents β. Some of the lately reported results do find some consistency in β. For example, both the MC and Langevin dynamics (LD) simulations were reported to give $\beta=2\nu$ for short and $\beta=1+\nu$ for long polymers in two dimensions, where ν is the swelling exponent [12,13]. Strictly universal scaling was claimed in [11], where $\beta=1.5$ was obtained both in two and three dimensions.

In addition, several computational investigations have suggested nearly linear scaling ($\beta=1$). On one hand, this close-to-linear behavior is prone to appear at the overdamped (i.e., Brownian) limit without self-avoiding effects, as shown by MC simulations in [14]. On the other hand, in [15] a β value close to unity could be inferred, but the polymer chains were found to be clearly out of equilibrium both on *cis* and *trans* sides in Brownian dynamics simulations, which was ignored in the interpretation of the results. Linear scaling has also been obtained from MC simulations in [16] and from an LD simulation [17], albeit for moderate ranges of N.

Not only do the different computational results and accompanying theories contradict, but they also seem to have very little to offer in explaining the available experimental

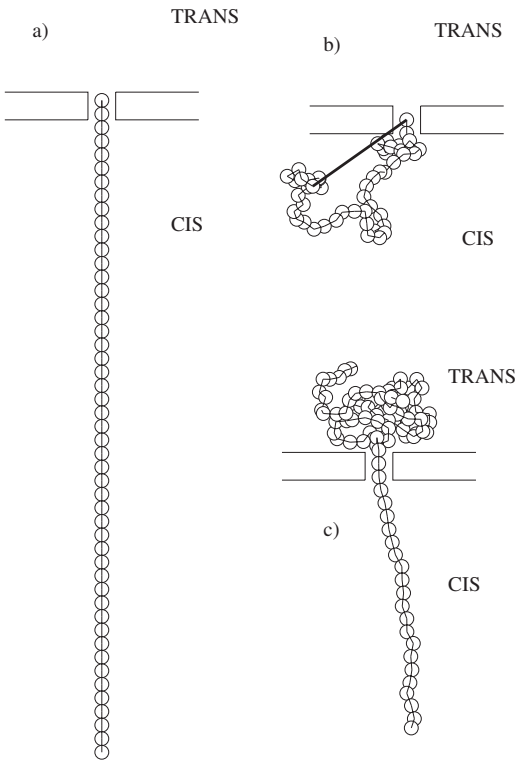

FIG. 1. Snapshots from three-dimensional (3D) Langevin dynamics simulations. (a) A straight initial configuration of a chain with $N=50$ beads. (b) A relaxed equilibrium initial configuration of a chain with $N=50$ beads. The wide solid line is the pore-to-end distance R_{pe}. (c) A chain with $N=100$ beads translocating with a force of $f/D_0=2.91$, when $s=80$ beads have translocated.

results. For example, the experimental study by Storm *et al.* [18] reports $\beta=1.27$, whereas the framework based on the fractional Fokker-Planck equation (FFPE) [10,11] claims uniform scaling different from this at all forces and is thus obviously in trouble here. Since there logically exists a requirement for the results obtained by using more realistic computational methods to be validated not only against experimental results but also against results from MC model simulations, a demand is placed for identifying the limitations and possible errors of the MC based translocation models.

Our recent study using molecular-dynamics-based simulations showed that β depends on the pore force and that the obtained values for β are in accord with the experiments [5]. As pointed out by Storm *et al.* [18], the experimental pore force magnitudes are anticipated to be larger than those used in computer simulations, which would explain the differing β values. However, larger force magnitudes in the MC method have been claimed to produce the same scaling relations as smaller ones. We suggest that saturation of transition probabilities for large forces in the MC method could be responsible for this discrepancy between simulated and experimental β values [18–23].

Accordingly, we set out to study the forced polymer translocation with the pore force f as a control parameter. Three different methods will be used for modeling the process. The standard MC method using Metropolis sampling will be compared with the kinetic (or n-fold) Monte Carlo method (KMC) [24,25] in one dimension. This comparison is made in order to characterize the forced translocation process. Differences between MC and KMC results would indicate subtleties in the effective independence of the events comprising the system [26]. LD simulations will be used as a reference in one dimension. With the LD method we also compute results in two and three dimensions to gain further evidence for our description of the forced polymer translocation. Finally, we determine the effect of the initial configuration on the scaling of the translocation time τ. In order to be free from potential artifacts due to spatial discretization, all results are produced by off-lattice simulations.

II. BACKGROUND

The investigation of the dynamics of forced translocation is subtly related to the assumption of close-to-equilibrium dynamics. The classic treatments of the problem by Sung and Park [6] and Muthukumar [7] assumed that a free energy F_s could be written down for the two ensembles on either side of the wall, when s segments have been translocated:

$$\frac{F_s}{k_BT} = (1-\gamma)\ln[s(N-s)] - \frac{s\tilde{f}\Delta z}{k_BT}, \tag{1}$$

where $\tilde{f}$ is the pore force, and $\gamma=0.69$ for a self-avoiding chain [7]. By using the free energy one can write down the one-dimensional Langevin equation for translocation as a function of translocation coordinate s when entropic effects are assumed small:

$$m\dot{s} = -m\xi\partial F_s/\partial s + \eta(t) = -m\xi\tilde{f}\Delta z + \eta(t), \tag{2}$$

where m, ξ, $\eta(t)$, and Δz are the bead mass, friction constant, random force, and pore length, respectively. From the Langevin equation the scaling of the translocation time with the pore force $\tau\sim f^{-1}$ is straightforwardly obtained, where $f \equiv \tilde{f}b/k_BT$ and b are the dimensionless pore force and the Kuhn length, respectively. Although the form of the Langevin equation [Eq. (2)] is identical in forced and unforced translocation, the connection between the free energy F_s and the pore force $\tilde{f}$ breaks down in forced translocation, where the pore force is a control parameter. The Langevin equation approach yields $\tau\propto N^2$ and $\tau\propto N^1$ as bounds for the translocation time scaling [7,9]. Based on mere unhindered motion of polymers over potential difference $\Delta\mu\sim f$ and the initial equilibrium configuration, Kantor and Kardar predicted that the translocation time should scale as [9]

$$\tau \sim \frac{N^{1+\nu}}{f}. \tag{3}$$

By the computational method where the polymer follows detailed molecular dynamics and the solvent coarse grained stochastic rotation dynamics, we have previously found that the translocating polymers are driven increasingly out of equilibrium on both sides of the pore under pore force magnitudes relevant in biological and experimental systems [5]. The dynamics is then mainly determined by the force balance between the drag force exerted on the mobile beads on the *cis* side and the constant pore force, $f_d=f$. Additional contribution comes from the crowding of the polymer beads on the *trans* side due to relaxation towards equilibrium being slower than the rate at which new segments enter through the pore. On the *cis* side the rate at which polymer beads are set in motion towards the pore was seen to be greater than the rate at which beads entered the pore, which indicates that the tension spreads along the polymer faster than what the polymer is able to relax towards equilibrium. By measuring the rate at which the tension spreads, an estimate could then be made for the scaling of the translocation time with the polymer length. We will present these observations in the Results section obtained from the LD method that, due to the absence of hydrodynamics, shows these characteristics even more clearly.

III. POLYMER MODEL

In the model system adjacent monomers are connected with anharmonic springs, described by the finitely extensible nonlinear elastic (FENE) potential,

$$U_{FENE} = -\frac{K}{2}R^2\ln\left(1-\frac{(l-l_0)^2}{R^2}\right). \tag{4}$$

Here l is the length of an effective bond, which can vary between $l_{min}<l<l_{max}$, $R=l_{max}-l_0=l_0-l_{min}$, and l_0 is the equilibrium distance at which the bond potential takes its minimum value. Choosing l_{max} as the unit length and $R=0.3$ yields $l_{min}=0.4$ and $l_0=0.7$. In the standard MC simulations $k_BT=1$ and the spring constant $K=40k_BT$. KMC dy-

namics proved more susceptible to bond fluctuations than standard MC dynamics, so $k_BT=0.1$ and $K/k_BT=400$ were used (see the next section). The FENE potential suffices in one dimension.

For two and three dimensions, where the LD method was used, the Lennard-Jones (LJ) potential,

$$U_{LJ}=4\epsilon\left[\left(\frac{\sigma}{r}\right)^{12}-\left(\frac{\sigma}{r}\right)^{6}\right], \quad r\leqslant 2^{-1/6}\sigma \tag{5}$$

$$U_{LJ}=0, \quad r>2^{-1/6}\sigma, \tag{6}$$

was used between all and the FENE potential, Eq. (4), between adjacent beads. The parameter values were chosen to be $\epsilon=1.2$ and $\sigma=1.0$ for the LJ, and $l_0=0$, $R=1.5=l_{max}$, $K=60/\sigma^2$ for the FENE potential. The used LJ potential with no attractive part mimics good solvent condition for the polymers. Initial states are relaxed equilibrium configurations.

IV. TRANSLOCATION MODELS

In one dimension we study the translocation dynamics using the MC, KMC, and LD methods. In order to link the 1D dynamics with forced translocation we define the segment s as translocated, when it passes the original position of the first bead. Time units cannot be expected to be identical for the three methods, but the scaling laws given by MC and KMC must be identical to those obtained from LD, if the MC and KMC methods are to be taken as representative models for forced translocation.

One-dimensional off-lattice Monte Carlo simulations are performed with the standard Metropolis acceptance test. A transition to a new state is attempted by picking at random a bead, computing the change in the particle's potential energy resulting from an attempted trial move by a distance δ from its present position r, $\Delta U=U(r+\delta)-U(r)$. Transition is always accepted for $\Delta U<0$, and according to its Boltzmann weight $\exp(-\beta\Delta U)$, if $\Delta U>0$. Time is incremented after each attempt, whether accepted or rejected, by a constant amount Δt. For a detailed pseudocode, see Appendix A.

Unlike in the Metropolis MC method, in the KMC algorithm the system is moved to another state at every attempt, regardless of how improbable the transition is. Accordingly, KMC has been the choice for doing simulations at low temperatures, where transition probabilities are low and, accordingly, Metropolis MC prohibitively slow. On the other hand, the additional bookkeeping required in KMC makes it computationally slower than MC at higher temperatures. However, MC and KMC have profound differences in other aspects than just computational efficiency.

In KMC the probability of the move is reflected on the (stochastically) estimated time Δt for the transition to take place, see Appendix B. Estimation of the elapsed time involves computing the system's all transfer probabilities, or rates, p_j, from which a cumulative function $R_i=\Sigma_{j=1}^{i}p_j$ is calculated. R_i is a class including events, whose probabilities $p_j\in(p_i^{min},p_i^{max}]$. From the possible transitions j the event to take place is picked at random, so that $R_{i-1}<uR(t)<R_i$, where $u\in(0,1]$ is a random number and $R(t)=R_l$ and l is the number of transition classes. The time elapsed between the previous and current event is estimated as $\Delta t=-1/R(t)\ln u'$, where $u'\neq u$ is a random number. It is noteworthy that the stochastically determined time increment Δt is inversely proportional to the the total probability, i.e., the rate of change $R(t)$ of the system evolving in time, here the instantaneous polymer configuration.

Due to finite distance for the trial move δ the Metropolis MC inevitably eliminates very improbable moves, which in the case of our 1D polymer simulations are those stretching or compressing polymer bonds far from their equilibrium lengths l_0. Hence as seen in our simulations, bond length fluctuations are larger in KMC than in MC. To maintain stability we used a lower temperature in our KMC simulations. A mere scaling of the bond potential magnitude by reducing the temperature does not change the dynamic universality class of the system.

Our LD algorithm was implemented according to [27]. The LD translocation algorithm was used also in two and three dimensions. In the algorithm, the pore force f is a free control parameter and not derived from free energy, as was done in Eq. (2). In the initial states the bond lengths are equal to relaxation distances and the first bead is in the middle of the pore. The pore diameter is $1.2b$ and length $3b$, where $b=1$ is the Kuhn length of the modeled polymer. We have used $k_BT=1$, $\xi=0.73$, and $m=16$ parameters in the Langevin implementation. This yields $D_0\equiv k_BT/\xi m\approx 0.086$ for the one-particle self-diffusion constant in one dimensional.

V. RESULTS

Our motivation for evaluating MC based methods in the context of forced translocation comes on one hand from discrepancies between scaling relations $\tau\sim N^{\beta}$ obtained from different MC simulations and on the other hand discrepancy between all MC simulations and experiments. We also look into the observed separate scaling regimes for short and long polymers. We base our evaluation of the methods mainly on the scaling of the translocation time with pore force and with polymer length. Since we take LD as the reference for the physical translocation system when hydrodynamic interactions are ignored, we first check these scaling relations using LD.

Figure 2(a) shows the scaling of the translocation time with respect to the dimensionless pore force $\tau\sim f^{\alpha}$ obtained from LD simulations in two and three dimensions. The thermal energy k_BT was kept fixed in all simulations. We obtained $\alpha=-0.990\pm0.01$ in two dimensions and $\alpha=-0.978\pm0.02$ in three dimensions. So, the scaling in these dimensions is the expected $\tau\sim f^{-1}$ in accordance with Eq. (2), confirming that entropic effects are weak.

Figure 2 shows the scalings of the translocation time with respect to chain length, $\tau\sim N^{\beta}$, for a frictional and frictionless pore in two dimensions in Fig. 2(b) and in three dimensions in Fig. 2(c). The scaling exponents β, identical for longer chains with frictional and frictionless pores, are shown in Table I for different values of f/D_0. There is a fair

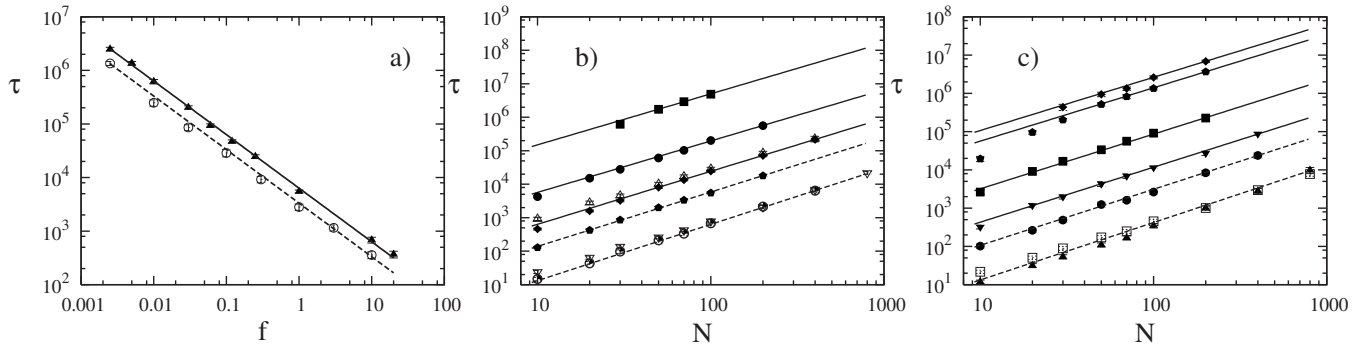

FIG. 2. (a) The scaling of the translocation time τ with respect to the external force f. Results from two dimensions (▲) and three dimensions (○) Langevin dynamics simulations yield the same $f \sim N^{-1}$ scaling. Since the simulations were done with the only difference in dimension, we note that in higher dimension the translocation process is faster. (b) 2D and (c) 3D Langevin dynamics simulation results for the scaling of the translocation time τ with respect to chain length N with various forces. Open symbols are with frictional pore and full symbols are with a ballistic pore. All plots yield different values for the scaling exponent β which are reported in Table I along with their corresponding forces. The finite size effect due to the frictional is identical to the 1D case (see text). With $f=10$ only chains with $N \geqslant 200$ follow the asymptotic scaling behavior. If the pore is nonaqueous (i.e., ballistic) the finite size effect applies only for chains smaller than $N=30$, and is amplified by reducing the force.

agreement between our 2D scaling exponents and those reported previously [13]. Qualitatively, the change of β with N with the frictional pore agrees with the aforementioned LD results where two scaling regimes were claimed. Accordingly, we obtain a smaller β for shorter chains. However, a quite different behavior is seen in the case of a frictionless pore. At a large enough force there exists only one scaling identical to the common scaling obtained for long polymers with both pores. Hence the translocation times longer than what would be expected from this scaling seem to be due to friction in the confined region inside the pore.

The scaling exponents β obtained in two dimensions, while agreeing with the results in [13], seem to be in strong disagreement with the scaling $\beta=1.53$ obtained by 2D MC simulations for an infinite potential with the pore length $\Delta z=1$. In addition, in another MC simulation in two dimensions $\beta=1.70$ has been obtained for two different forces $f=1,5$ with $\Delta z=3$ [12]. So, not only do MC results contradict with LD results, but MC simulations mutually disagree. To check if this could be due to the MC translocation model possibly belonging to a different dynamic universality class from the respective LD model we simulated the simplest possible case, i.e., 1D forced translocation using KMC in addition to MC and LD. We obtain invariably $\beta=2$ for LD, MC, and KMC, in agreement with the previous MC result [9], so the computational MC model using Metropolis sampling seems to produce correct time dependence, although forced translocation can hardly be taken as a purely Poissonian process [26]. However, we do find a method-dependent artifact which explains the apparent discrepancy.

TABLE I. Langevin dynamics. Values of β obtained from Fig. 2. Here $U=\tilde{f}\Delta z/k_BT$ is the dimensionless pore potential.

U	f/D_0	β ($d=2$)	β ($d=3$)
0.0036	0.014	1.52 ± 0.08	1.40 ± 0.04
0.0075	0.03		1.40 ± 0.02
0.03	0.35	1.54 ± 0.03	1.43 ± 0.02
0.75	2.91	1.58 ± 0.01	1.44 ± 0.03
3	11	1.63 ± 0.04	1.47 ± 0.05
30	116	1.68 ± 0.02	1.50 ± 0.01

Also in one dimension the translocation time obtained from LD simulations is found to scale with the pore force as $\tau \sim f^{-1}$; Fig. 3(a). MC and KMC models also give this scaling with pore force $f<1$. However, for $f \geqslant 1$ the translocation time levels off to a constant value. Potentially, KMC might not be as sensitive to this artifact, as will be discussed in more detail later. However, KMC algorithm fails to run with so large a force, due to the above-explained higher probability of moving a particle regardless of whether a bond breaks or not. In two dimensions the breaking of the force scaling has been reported in MC forced translocation simulations in two [12] and three [16] dimensions. Our simulations strongly imply that it is related to the saturation of the transition probabilities in MC at large force values inside the pore (see Appendix A, step 6).

The discrepancy between the different β values obtained from MC simulations can be explained by this artifact related to Metropolis sampling. The infinite force for which $\beta=1.53$ was obtained [9] takes the MC model to the plateau region ($f>1$), where $f=\infty$ is no different from $f=1$ in that it gives identical velocity v to the translocating polymer, when the pore length Δz is constant. However, by increasing Δz while keeping the force acting per polymer bead f constant, does increase pore potential and thus the polymer velocity v which in turn, according to our simulations, increases β (see Fig. 2 and Table I). The pore potential ΔU over the pore is explicitly shown to be the primary control parameter for forced translocation in Table II, where translocation times are compared when either the force acting on polymer beads inside the pore or the pore length is changed in the LD model. In [9] $\Delta z=1$, while in [12] $\Delta z=3$ was used. Of the two force values $f=1,5$ in [12] the latter is within the plateau regime and the first at least very close to it, which would explain the obtained almost identical β values. Due to $f=\infty$

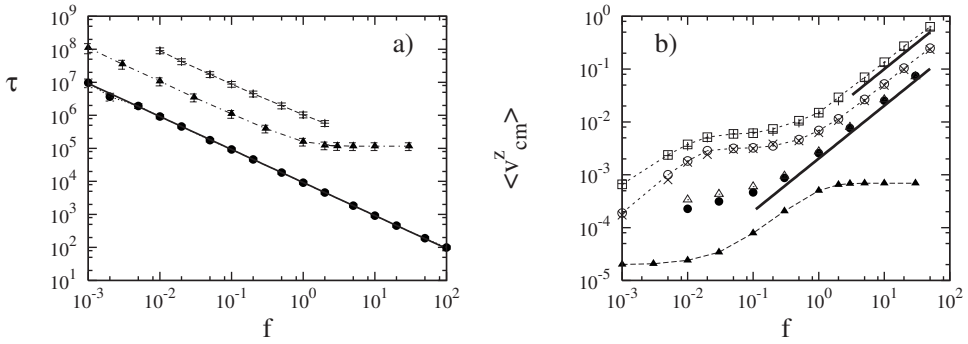

FIG. 3. (a) Comparison of the scaling of translocation time τ (in arbitrary units) with pore force f in one dimension obtained from MC (▲), KMC (×), and LD (●) simulations. Polymers are of constant length $N=50$. All computational methods yield the same force scaling $\tau \sim f^{-1}$ for $f \leqslant 1$. The MC method shows an artifact in the force regime $f \gg 1$. KMC fails to perform in this regime (see text). (b) The average center-of-mass velocity in the z direction, $\langle v_{cm}^z \rangle$, as a function of the dimensionless pore force f, for $N=20$ (+, □) and $N=50$ (×, ○) in one dimension, for $N=100$ (●) in two dimensions, and for $N=100$ (△) in three dimensions. The data for (□) and (○) were obtained using a frictionless pore in LD simulations. All other results are from LD simulations using a frictional pore. Linear scaling is plotted as a solid line to guide the eye. At the bottom, results from 1D MC simulations (▲) with $N=50$ are shown (in arbitrary units). See the text for details.

being in effect just the constant force value in the plateau regime, ΔU in [9] is lower than what was used in [12], which explains why this β value for the infinite force is lower than what was obtained for force values 1 and 5. The saturation of the transition probabilities could also be the reason why in three dimensions MC simulation results presented in [11] to support FFPE predictions the value of β did not change, when the pore force was varied. Hence it would seem that there is no reason to assume a universal β for all f.

The prevailing discrepancy between simulations can be at least partly explained by the deficiency of the MC method at large force regime, which is the biologically and experimentally relevant force range. For example, the Kuhn length of the single-stranded DNA (ssDNA) $\tilde{b}=1.6$ nm, and a charge density $1.28e/\text{nm}$ reported in [28] for free ssDNA in an ionic solvent would result in the effective charge of $2\ e/\tilde{b}$. Taking into account that the pore is prone to screen the charges even more than the solvent [29] the effective charge on a nucleotide traversing the pore was estimated to be $\approx 0.1e$. In the α-hemolysin pore of length 5.2 nm there are approximately 13 nucleotides of length 0.4 nm [30], yielding total effective charge $q^*=1.3e$ for the polymer segment inside the pore. The typical experimental pore potential is $V \approx 120$ mV [18–21]. At $T=300$ K, the dimensionless ratio $U=q^*V/k_BT \approx 6.03$ is obtained, which corresponds to the dimensionless value $U=\tilde{f}\Delta z/k_BT$. Accordingly, the corresponding dimensionless force $f=\tilde{f}b/k_BT$ has a value of $\simeq 2$ in our MC simulations, which is already well in the plateau regime; see Fig. 3(a).

TABLE II. Results from 3D Langevin dynamics for a polymer of length $N=100$. Here $\Delta U \approx f\Delta z/k_BT$ is the dimensionless potential over the pore.

ΔU	f	Δz	τ
30	10	3	326 ± 10
15	10	1.5	642 ± 20
30	20	1.5	354 ± 10

We checked the effect of the pore friction in one dimension, where dynamics is no more constrained inside than outside the pore, making comparison of the cases with frictional and frictionless pores straightforward. The same characteristics as in higher dimensions were seen. With a frictional pore $\beta=2$ is obtained only for $N \geqslant 30$. From 1D LD simulations with a frictional pore this maximum length l_{max} was seen to increase with pore force f. Increasing f increases the average velocity of the polymer $\langle v \rangle$ and so increases frictional contribution. Since the force acts only on the part of the polymer inside the pore, at large enough force frictional term damps movement only in the direction from the *cis* to *trans* side thus increasing the translocation time proportionately more for short than long polymers. At a very weak force this effect is not perceived due to friction affecting movement in both directions (i.e., also from *trans* to *cis*), as seen also in dimensions 2 and 3 from the topmost curves in Figs. 2(b) and 2(c). This is by definition a finite-size effect and bound to affect the obtained β more for shorter polymers, where the portion in the pore constitutes a larger part. The decrease of β due to pore friction is understandable, since in the asymptotic limit of completely friction-dominated dynamics linear scaling, $\beta=1$, with polymer length is to be expected.

We measured the center-of-mass velocity $\langle v_{cm}^z \rangle$ in the z direction, which is the direction perpendicular to the wall from *cis* to *trans*, with a frictional and frictionless pore; see Fig. 3(b). Comparing the 1D curves obtained from LD and MC in Figs. 3(a) and 3(b) it is clear that $\langle v_{cm}^z \rangle$ is not simply reciprocal of τ, which indicates that one must be cautious in applying equilibrium concepts and observables in characterizing translocation. Based on this finding, using $\langle z_0 \rangle / \tau$, where z_0 is the z coordinate of the last polymer bead in the initial equilibrated configuration, is not equivalent to using $\langle v_{cm}^z \rangle$ for translocation velocity. In one dimension it is particularly clear that the first definition simply sets the translocation velocity $v \sim 1/\tau$, a valid definition for translocation velocity, but one that also easily leads to drawing wrong conclusions about translocation dynamics. Comparing Fig. 2(a) and 3(b), the same characteristics is seen in dimensions

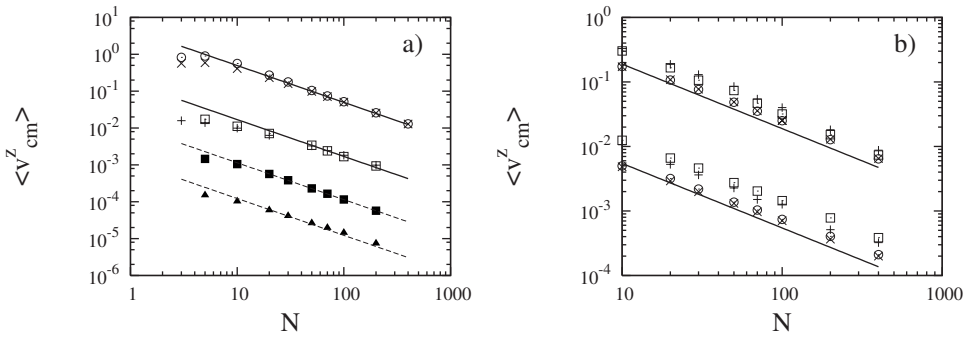

FIG. 4. This (a) The average center-of-mass motion along the translocation coordinate $\langle v_{cm}^z \rangle$ as a function of the chain length N in one dimension, with Langevin dynamics. Two different pore forces $f=0.1$ (+, □) and 20 (×, ○) have been used. Both frictional (+, ×) and frictionless (□, ○) pores were used. MC results in one dimension with $f=0.1$ (▲) and 20 (■) are also shown (in arbitrary units). The solid and dashed lines have a slope of −1. (b) $\langle v_{cm}^z \rangle$ as a function of the chain length N. Results are from Langevin dynamics simulations in two dimensions (□, ○) and three dimensions (+, ×), with two different pore forces $f=0.25, 10$ for the lower and higher points, respectively. Both frictional (+, □) and frictionless (×, ○) pores were used. The solid lines $\sim 1/N$ are plotted to guide the eye.

2 and 3. From Fig. 3(b) it is seen first of all that the artifact in MC at large force magnitudes manifests itself in $\langle v_{cm}^z \rangle$ measured in the 1D system. Outside of that, the $\langle v_{cm}^z(f) \rangle$ curves for 1D MC and LD are qualitatively fairly similar. The additional regime at very weak force magnitudes in LD was checked to be related with the form of the FENE potential, showing distinctively in one dimension where it is the only potential between polymer beads.

To make sure that we are seeing finite-size effects for short polymers with a frictional pore instead of two scaling regimes for short and long polymers, we also check the dependence of $\langle v_{cm}^z(f) \rangle$ on polymer length N. In accord with the findings in [9] the center-of-mass motion of a polymer translocating through a pore closely conforms to *unimpeded motion*, where $\langle v_{cm}^z \rangle \sim 1/N$ with both the frictional and frictionless pore; see Fig. 4. It is evident that pore friction does not affect the behavior of $\langle v_{cm}^z \rangle$ that is a measure of the transfer of the whole polymer. Hence the differences in Figs. 2(b) and 2(c) have to come solely from the frictional contribution to the finite portion of the chain in the pore. The effect is seen clearly in τ that is a local observable quantifying the transfer of the segments over the pore.

The above observation that $\langle v_{cm}^z(f) \rangle \nsim 1/\tau(f)$ indicated that the transfer of the part of the polymer crucial for characterization of forced translocation, i.e., the part in the vicinity of the pore does not remain even close to thermal equilibrium. Any meaningful description of the translocation process must then succeed to capture the mechanics of this part. Given that any diffusive, or close-to-equilibrium description is invalid, the remaining minimum condition is force balance. Indeed, it turns out that the observed scaling behavior $\beta \leqslant 1+\nu$ in two and three dimensions can be explained by the force balance of the drag force exerted on the mobile beads on the *cis* side and the constant pore force, $f_d=f$. Just as in [5] we measured the squared distance $R_{pe}^2(n)$ [see Figs. 1(b) and 5], of the polymer bead n from the pore on the *cis* side during translocation, see Fig. 6(a), from which the segments toward the free end of the polymer are seen to remain immobile until they are pulled toward the pore. Figure 6(b) shows that the number of mobile beads increases linearly as a function of translocated beads, $s_m=ks$. Up to lengths of $N \approx 100$, $k \sim N^{-\chi}$, beyond which it gradually levels off to a constant value greater than unity. The mobile beads comprise a moving segment, which already for moderate pore force exhibit no folding indicating that the relaxation of the beads in the moving segment is far slower than the rate at which they are translocated, see Figs. 1(c) and 5. f_d is exerted on the mobile beads, so $f_d \sim s_m \langle v \rangle$, where $\langle v \rangle$ is the average velocity of the mobile beads. When the whole chain has translocated, $f_d \sim N_m \langle v \rangle$, where $N_m=kN$. The beads are set in motion from their equilibrium positions, so the distance d of the last bead to be translocated scales as $d \sim N^{\nu}$. The average translocation time then scales as $\tau \sim \langle d \rangle / \langle v \rangle \sim kN^{1+\nu} \sim N^{1+\nu-\chi}$. For example, for $f/D_0=2.9$, we obtain $\chi \approx 0.3$ from the data displayed in Fig. 6(b), which would give $\beta \approx 1.3$. The crowding of polymer beads close to the pore on the *trans* side [see Fig. 1(c)] increases β from this value. The crowding increases with force, which has been shown in [5]. From Fig. 6(b) it can be seen that k saturates when f is increased, which also increases β at large f.

In order to confirm that the presence of ν in the scaling exponent $\beta=1+\nu$ comes solely from the initial configuration and not from any factor due to close-to-equilibrium motion and Rouse relaxation time, we check the scaling and the

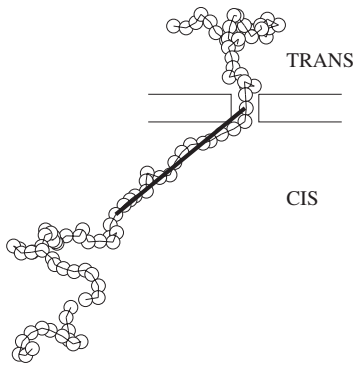

FIG. 5. A snapshot at $s=35$ of a 3D LD simulation with a polymer of length $N=100$. The dimensionless pore force used here is $f=0.01$. The wide solid line represents the pore-to-end distance R_{pe} as the number of mobile beads s_m reaches the index of the observed bead, $n=52$.

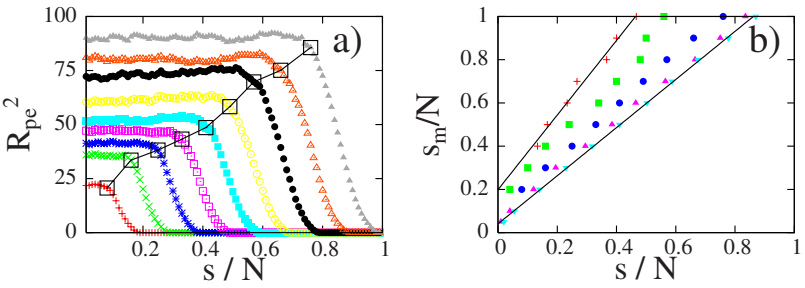

FIG. 6. (Color online) (a) 3D Langevin dynamics. Averaged squared distances of beads numbered 30, 50, 70, 100, 200, and 400 from the pore as a function of the number of translocated beads s for polymers of length $N=100$. The force $f=0.25$. (b) The number of mobile beads s_m vs the number of translocated beads s, both normalized to the polymer length N.

average waiting time $t(s)$ for the segment s to translocate for an initially extended configuration; Fig. 1(a). We obtain $\beta=2$ for this initial configuration. The average waiting time profiles of the initially extended and equilibrated configurations are shown in Fig. 7. For the initially extended configuration we obtain linear dependence $t(s)\sim s$ giving exactly the obtained scaling with $\beta=2$. Hence the upper limit for the scaling exponent β results from the waiting times of the translocating beads, determined solely on their initial positions. In other words, already with a moderate pore force translocation velocity completely dominates the process so that diffusive motion has no effect and the the only prevailing condition governing translocation dynamics is the force balance described above.

VI. SUMMARY

We have studied forced translocation without hydrodynamics in different dimensions using Monte Carlo (MC), kinetic Monte Carlo (KMC), and Langevin dynamics (LD) methods. We have shown that the forced translocation model using MC with basic Metropolis sampling gives the correct time dependence at moderate pore potentials but presents an artifact at large pore potentials. This artifact seems to explain the prevailing controversy between different MC results. It also seems to account for results claiming universal scaling of the translocation time with the polymer length, $\tau\sim N^{\beta}$, independent of the pore force magnitude and hence the prevailing discrepancy between computational and experimental findings on forced translocation.

Using LD in two and three dimensions we have shown that the scaling exponent β increases with the pore force f. We obtain $\beta=1+\nu$ as the high force limit. By measurements of polymers' center-of-mass velocities we have shown that description of forced translocation with concepts related to close-to-equilibrium concepts is not well founded. We have given a description of the forced translocation based on simple force-balance condition, where the drag force exerted on the part of the polymer on the *cis* side changes with the number of polymer beads in motion. This description gives the above upper limit for β and also explains the increase of β with f. We have also shown that crowding of polymer beads is strong in the vicinity of the pore on the *trans* side.

ACKNOWLEDGMENT

This work has been supported by the Academy of Finland (Project No. 127766).

APPENDIX A: METROPOLIS MONTE CARLO ALGORITHM

1. Choose an initial state, and set the time $t=0$.
2. Randomly choose a particle with label i, and calculate a trial position $\vec{r}_i'=\vec{r}_i+\vec{\delta r}_i$.
3. Calculate the energy change, $\Delta U=-\vec{f}_i\cdot\frac{\vec{\delta r}_i}{|\vec{\delta r}_i|}+U_{FENE}(\vec{r}_i+\vec{\delta r}_i)-U_{FENE}(\vec{r}_i)$, resulting from this displacement.
4. If $\Delta U<0$, the move is accepted; go to step 2.
5. Get a uniform random number $u\in(0,1]$.
6. If $u<\exp(-\Delta U/k_BT)$, accept the move.
7. Update the time $t=t+1/N$ and go to step 2.

APPENDIX B: KINETIC MONTE CARLO ALGORITHM

The KMC algorithm for simulating the time evolution of a system where some processes occur with known average rates, or probabilities, $p_i=\exp(-\Delta U)$, where ΔU is as defined in Appendix A, can be written as follows:

1. Choose an initial state, set the time $t=0$, and form a list of all possible rates in the system p_i.
2. Calculate the cumulative function $R_i=\Sigma_{j=1}^{i}p_j$ for $i=1,\ldots,l$, where l is the total number of transitions. Denote $R=R_l$.
3. Get a uniform random number $u\in(0,1]$.
4. Find the event to carry out by finding the i for which $R_{i-1}<uR<R_i$.

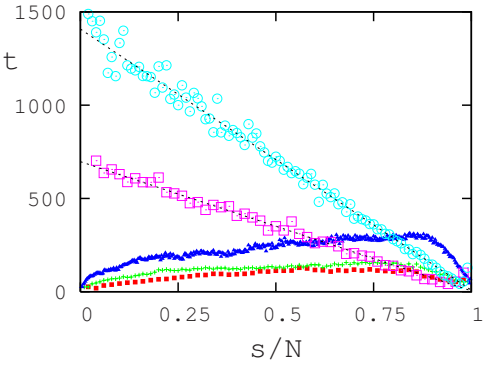

FIG. 7. (Color online) 3D LD. Waiting time averages $t(s)$ as a function of the translocated segment s with $f/D_0=2.91$. Profiles with filled ($N=50$: ■, $N=100$: ●, $N=400$: ▲) and empty symbols ($N=50$: □, $N=100$: ○) represent runs with an equilibrium initial configuration and with a straight initial configuration, respectively. Note that the latter profiles yield a clear linear behavior.

5. Carry out event i.

6. Recalculate all rates p_i which may have changed due to the transition. If appropriate, remove or add new transitions i. Update N and the list of event rates accordingly.

7. Get a new uniform random number $u' \in (0,1]$.

8. Update the time with $t=t+\Delta t$, where $\Delta t=-\frac{\ln u}{R}$.

9. Return to step 2.

(Note that the same average time scale can be obtained also using $\Delta t=\frac{1}{R}$ in step 8. However, including the random number describes better the stochastic nature of the process.)

This algorithm is known in different sources variously as the residence-time algorithm or the n-fold way or the Bortz-Kalos-Lebowitz (BKL) algorithm or just the kinetic Monte Carlo (KMC) algorithm.

[1] I. Ali and J. M. Yeomans, J. Chem. Phys. **123**, 234903 (2005).
[2] M. Fyta, E. Kaxiras, S. Melchionna, and S. Succi, Comput. Sci. Eng. **2**, 20 (2008).
[3] M. Bernaschi, S. Melchionna, S. Succi, M. Fyta, and E. Kaxiras, Nano Lett. **8**, 1115 (2008).
[4] M. G. Gauthier and G. W. Slater, Eur. Phys. J. E **25**, 17 (2008).
[5] V. V. Lehtola, R. P. Linna, and K. Kaski (to be published).
[6] W. Sung and P. J. Park, Phys. Rev. Lett. **77**, 783 (1996).
[7] M. Muthukumar, J. Chem. Phys. **111**, 10371 (1999).
[8] J. Chuang, Y. Kantor, and M. Kardar, Phys. Rev. E **65**, 011802 (2001).
[9] Y. Kantor and M. Kardar, Phys. Rev. E **69**, 021806 (2004).
[10] J. L. A. Dubbeldam, A. Milchev, V. G. Rostiashvili, and T. A. Vilgis, Phys. Rev. E **76**, 010801(R) (2007).
[11] J. L. A. Dubbeldam, A. Milchev, V. G. Rostiashvili, and T. A. Vilgis, Europhys. Lett. **79**, 18002 (2007).
[12] K. Luo, I. Huopaniemi, T. Ala-Nissila, and S.-C. Ying, J. Chem. Phys. **124**, 114704 (2006).
[13] I. Huopaniemi, K. Luo, T. Ala-Nissila, and S.-C. Ying, J. Chem. Phys. **125**, 124901 (2006).
[14] M. G. Gauthier and G. W. Slater, J. Chem. Phys. **128**, 205103 (2008).
[15] P. Tian and G. D. Smith, J. Chem. Phys. **119**, 11475 (2003).
[16] H. C. Loebl, R. Randel, S. P. Goodwin, and C. C. Matthai, Phys. Rev. E **67**, 041913 (2003).
[17] C. Forrey and M. Muthukumar, J. Chem. Phys. **127**, 015102 (2007).
[18] A. J. Storm, C. Storm, J. Chen, H. Zandbergen, J.-F. Joanny, and C. Dekker, Nano Lett. **5**, 1193 (2005).
[19] J. J. Kasianowicz, E. Brandin, D. Branton, and D. W. Deamer, Proc. Natl. Acad. Sci. U.S.A. **93**, 13770 (1996).
[20] A. Meller, J. Phys.: Condens. Matter **15**, R581 (2003).
[21] J. Li, M. Gershow, D. Stein, E. Brandin, and J. A. Golovchenko, Nature Mater. **2**, 611 (2003).
[22] L. B. Chen, Annu. Rev. Cell Biol. **4**, 155 (1988).
[23] S. Huang, K. S. Ratliff, and A. Matouschek, Nat. Struct. Biol. **9**, 301 (2002).
[24] W. M. Young and E. W. Elcock, Proc. Phys. Soc. London **89**, 735 (1966).
[25] A. B. Bortz, M. H. Kalos, and J. L. Lebowitz, J. Comput. Phys. **17**, 10 (1975).
[26] K. A. Fichthorn and W. H. Weinberg, J. Chem. Phys. **95**, 1090 (1991).
[27] M. Allen and D. J. Tildesley, *Computer Simulation of Liquids* (Oxford Science Publications, Oxford, 2006).
[28] M.-N. Dessinges, B. Maier, Y. Zhang, M. Peliti, D. Bensimon, and V. Croquette, Phys. Rev. Lett. **89**, 248102 (2002).
[29] A. F. Sauer-Budge, J. A. Nyamwanda, D. K. Lubensky, and D. Branton, Phys. Rev. Lett. **90**, 238101 (2003).
[30] A. Meller, L. Nivon, and D. Branton, Phys. Rev. Lett. **86**, 3435 (2001).